

Fabrication and Testing of a Medical Surgical Instrument Capable of Detecting Simulated Embedded Lumps

¹Javad Dargahi, ²Siamak Najarian, ¹Reza Ramezanifard and ³Farhad Tabatabai Ghomshe

¹ Department of Mechanical and Industrial Engineering, Concordia University, 1455 de Maisonneuve Blvd. West, Montreal, Quebec, Canada

²Department of Biomechanics, Artificial Tactile Sensing and Robotic Surgery Lab, Faculty of Biomedical Engineering, Amirkabir University of Technology, Tehran, Iran

³University of Social Welfare and Rehabilitation Sciences, Tehran, Iran

Abstract: A novel endoscopic grasper is being fabricated and tested. This grasper can be used in detecting lumps or tumors in biological tissues. The detailed fabrication process of the tactile sensor has been discussed. Custom-made sensors were integrated with the jaws of the endoscopic grasper and objects with known tactile features were tested by the designed grasper. Different experiments were performed with the system in order to determine both the position and the size of the lumps or inclusions located in the soft elastomeric media. The average discrepancy between the experimental and theoretical simulations was found to be less than 15%.

Keywords: Softness Measurements, Tumor Detection, Sensed Objects, Tactile Sensing

INTRODUCTION

Minimally access surgery, also known as minimally invasive surgery (MIS), is becoming very popular in new surgical procedures. These techniques have been developed to decrease the traumatic effects of various types of surgeries [1-5]. In this kind of operative procedure and unlike open surgeries, the surgeons cannot use their hands directly in manipulating the operation site. In other words, they do not have their hands inside the patient's body [6-9]. This means that various medical manipulations are not being performed in the operation sites. Therefore, the surgeons would have to use long slender instruments outside the operative zone and transmit the manipulations, such as grasping, cutting or other maneuvers to the sites by the hand tools [10]. Here, the surgical instruments pass through tiny holes pierced in the patient's skin. Although MIS has a considerable number of advantages, such as, less tissue damage, less postoperative pain, faster recovery period, fewer postoperative complications, and reduced hospital stay, it also suffers from several disadvantages [11-14]. These disadvantages include: loss of tactile sensing feedback, the need for increased technical expertise, a possibly longer duration of the surgery, and difficult removal of

bulky organs. The loss of tactile sensing feedback translates to the fact that the surgeons would not be able to feel the tissues. For instance, if there are any lumps or abnormal tissues in the background tissue, there is a possibility that the operators might easily miss them. At the same time, the risk of accidental cutting of the surrounding veins or arteries that are embedded in the tissues can lead to serious complications. Due to these problems, the loss of tactile sensing has proven to be a serious issue and has been the target of extensive research [15-19].

A tactile sensor with standing piezoresistive cantilevers embedded in an elastic material is being proposed [20]. The sensor detects the shear stress applied on its surface. Each standing piezoresistive cantilever in the elastic material detects a certain axial component of applied shear stress. By arranging this standing piezoresistive cantilever in orthogonal directions, the directions and the magnitudes of applied shear stress is detected. The concept of an inexpensive PVDF pyroelectric radiation sensor of large aperture is being described and the design details of the pyroelectric sensor based on the PVDF polymer are being given [21]. A micro-mechanical sensing platform is being described with which the various elastic properties of the ovum can be characterized using uniaxial

Corresponding Author: Prof. Siamak Najarian, No. 424, Hafez Avenue, Department of Biomechanics, Faculty of Biomedical Engineering, Amirkabir University of Technology, Tehran, Iran, P.O. Box 15875-4413.
Tel: (+98-21)-6454-2378. Fax: (+98-21)-6646-8186

measurements [22]. Novel textiles are being developed using conducting polymer coatings which are deposited on a foam substrate [23]. The foam they used is a soft, porous conductive solid made by chemically oxidizing pyrrole in the presence of a polyurethane foam. The resulting structure is sensitive to pressure exerted from all three dimensions making it attractive for use as wearable sensors for medical applications.

In order to improve the manipulation ability of endoscope, a new tactile sensor system using image processing has been developed [24]. As this system uses an infrared (IR) cut pattern, it is possible to install the sensor in the tip of an existing endoscope easily. In a research work, using a modified commercial endoscopic tool, the magnitude of the applied force was measured by strain gauges, and then the position of the grasper was determined with an optical detector [25]. They obtained force-displacement data and identified objects with five different elastic properties. A report has been published on compliance of a hard rubber embedded in a block of foam using remote palpation [26]. Additionally, an endoscopic and robotic micromachined sensor has been designed and fabricated using PVDF film [27]. Design, fabrication, and theoretical studies of a micromachined piezoelectric tactile sensor for an endoscopic grasper have been discussed [28]. The sensor exhibited high force sensitivity, high dynamic range, good linearity, and high signal to noise ratio. In another work, a force-moment sensor has been placed into the distal shaft of a laparoscopic forceps as well as a tactile sensor array between the jaws of the forceps [29]. The piezoresistive sensor array used was a foil sensor with 64 measuring points. Various attempts have been made to tackle the problem of reducing the number of sensors using PVDF films [30-32].

The development of an active haptic sensor for monitoring skin conditions has been discussed [33]. The base of the tactile sensor is an aluminum cylinder, around which a polyurethane rubber, a PVDF film, a protective surface layer of an acetate film and lace are stacked in sequence. Their experimental results show that the sensor system works well as a haptic sensor for monitoring skin conditions. A research has been published that discusses the preliminary tests and basic design parameters for single tactels using electrorheological fluids [34]. The final aim was to produce a prototype three-dimensional tactile display comprising electrically switchable micro-machined cells whose mechanical moduli are governed by phase changes experienced by electrorheological fluids. A micro-tactile sensor has been developed to measure

elasticity together with the instant of contact [35]. Using finite element modeling, they found a frequency where longitudinal and rotational vibration modes exist and used these results to signal touch detection.

Following the above-mentioned progress and our previous studies [36], the need for the design of a smart surgical tool that can display the map of the tissue interior is of great importance. This research work focuses on the construction of a novel type of endoscopic grasper, which can be used to convert the sense of touch into images readily recognizable by the surgeon. Using the proposed system, the surgeons can detect the presence or absence of unusual lumps (such as tumor) by simply grasping the suspicious organ by a smart endoscopic grasper. Simultaneously, the surgeon can have an estimate of both the size and position of the tumors or lumps by looking at the custom-designed gray scale display.

MATERIALS AND METHODS

Fabrication of sensor: This part describes the microfabrication processes used to fabricate the piezoelectric tactile sensor. The assembly of the sensor is also discussed. The tactile sensor consists of a silicon substrate with a PVDF film (Good Fellow Company, USA) sandwiched between the silicon substrate and the rigid and soft cylinders (see Fig. 1).

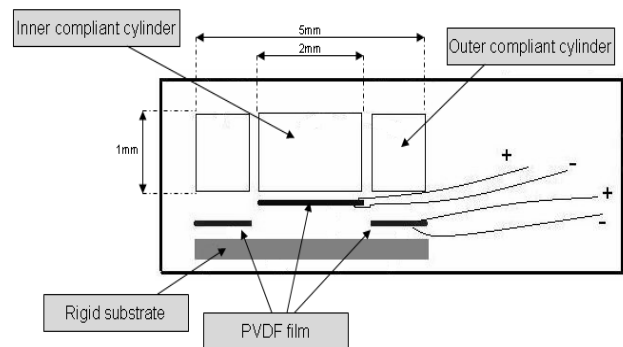


Fig. 1: Schematic representation of the sensor unit.

The geometrical size of the sensor was selected from the preliminary design calculations performed. Two designs, one with a single sensor and the other one with four sensors were realized. Both designs had a silicon substrate as the base. Silicon substrate, PVDF, Plexiglas and liquid silicone rubber were the materials involved in the fabrication of the sensor. The microfabrication process sequences of the sensor are described below.

Step 1 was the micromolding of the outer cylinders. The material used for micromolding of the outer cylinders of the tactile sensor was liquid silicone rubber (SYLGARD 184) which was purchased from Dow coming Inc. The desired shape was a hollow cylinder. To start with, we had to create a mold cavity of the required shape and size of 6 mm outer diameter, 4 mm inner diameter and 1mm depth. This cavity, in the shape of hollow cylinder, was achieved by very high precision machining. Once the cavity was created, the LSR which comes as a combination of base (octamethylcyclotetrasiloxane) and curing agent (dimethyl methylhydrogen siloxane) was mixed thoroughly in a beaker in a ratio of 10:1. During mixing of the base and curing agent, a lot of bubbles were created. To remove these bubbles, the base-curing agent mixture was de-aerated with the help of a vacuum pump. This process was repeated until all the bubbles were completely removed. Following this, the base curing agent mixture was carefully poured into the mold cavity. A few drops of Teflon were sprayed around the mold cavity for easy removal of the cured rubbers. Then, the mold cavity along with the LSR mixture was cured in an oven at a temperature of 150°C for 15 min. The general curing temperature and time for Sylgard 184 LSR are presented in Table 1.

Table 1: Curing time-temperature chart for Sylgard 184

Curing Temperature	Curing Time
Room temperature	48 hours
100°C	45 minutes
125°C	20 minutes
150°C	10 minutes

Once the curing process was over, the ring shaped liquid silicone rubber structures were released from the cavity. Thus, the final shape was realized which was of the order of 1 mm height as shown in Fig. 2.

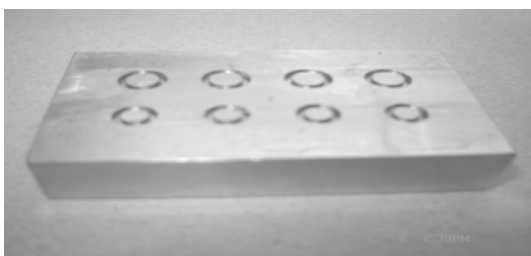


Fig. 2: Photograph of the fabricated mold cavity.

Step 2 was the construction of the inner rigid cylinders. These structures were made of Plexiglas,

which were machined to the required diameter of 3 mm and 1 mm height by high precision machining. Step 3 was the patterning of PVDF films to obtain the required cylindrical shape. UV light was directed through a mask to selectively expose photosensitive materials. We used a photolithography process in this step. The photolithography was conducted in a room illuminated yellow in color to reduce the adverse effects of light on the photosensitive resist material. Photoresist (PR) was applied on a wafer by spin coating. The coated wafer was then dried in an oven, exposed to UV light and then developed using a developer. The purpose of the photoresist was to protect chosen regions of the wafer for subsequent fabrication steps. A schematic depicting of this process is shown in Fig. 3.

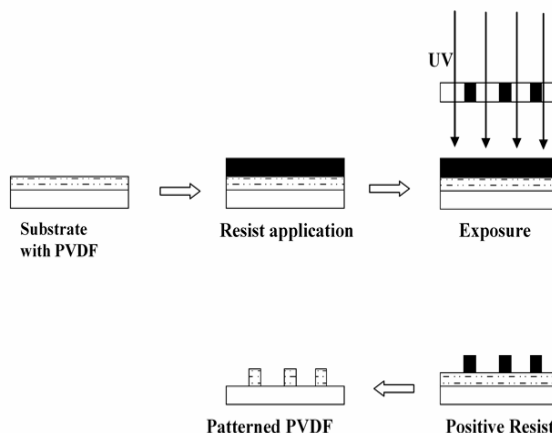


Fig.3: Schematic representation of the photolithography process.

The photolithography process employed for our sensor fabrication included: surface preparation, coating (spin casting), pre-bake (soft bake), alignment, exposure, development, post-bake (hard bake), and stripping of PR. Some of these processes are discussed below.

In surface preparation process, the PVDF film was glued onto a silicon wafer using the photoresist (PR). A bare silicon wafer was first cleaned and photoresist was spin coated on it. The photoresist here acts as glue for the PVDF on the silicon wafer. Subsequently, the PVDF film of the required size was cut and placed over the surface spin with photoresist. It was pressed so that the PVDF film gets glued to the substrate. Then, the substrate along with the PVDF was soft baked for 30 sec at 75°C on a hot plate. Following this, the PVDF was successfully glued to the silicon substrate.

In the spin coating process, the silicon wafer along with the PVDF film was held on a spinner chuck by

vacuum and photoresist was coated to uniform thickness by spin coating. Seven to eight drops of photoresist was dropped onto the PVDF film and the chuck was spun at a speed of 500 rpm for 15 sec and then at 3000 rpm for 30 seconds. By this method of spinning, we ensured that the photoresist was coated uniformly over the PVDF film. The resist thickness was set primarily by resist viscosity and by spinner rotational speed. Figure 4 shows the photograph of the spin coater setup.

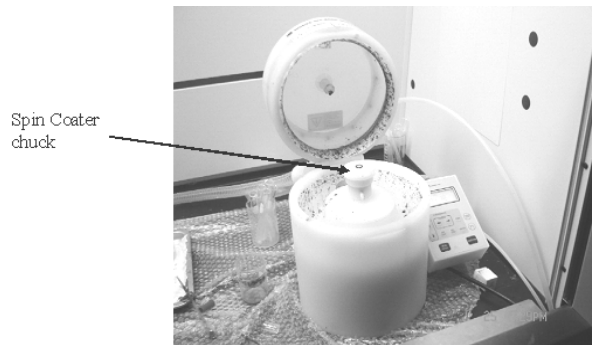


Fig. 4: Photograph of the spin coater set-up.

The next process was the soft bake. After the PR was spun on the PVDF film, we soft baked it in an oven. This process was done to evaporate the coating solvent and to densify the resist after spin coating. Typical thermal cycles were 50°C for 40 min in an oven and 75°C to 85°C for 45 sec on a hot plate. Once the sample was soft baked, the next procedure was to expose it to UV light through the predefined light field mask. Figure 5 shows the photolithography set-up used to pattern PVDF.

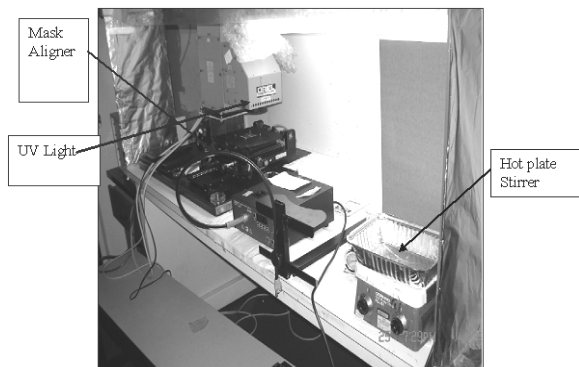


Fig. 5: Photolithography set-up.

Incorporation of the fabricated sensors: The single sensor used for study cannot serve the purpose of the

endoscope grasper mounting. Endoscopic graspers require a number of small micromachined tactile sensors mounted in the form of array. In practical applications, these sensors could be in number of 4 to 6 in a regular pattern of array. Even though, there could be different arrangements for assembling the sensor on the endoscope. Figure 6 shows the detailed drawing of the endoscopic grasper with 8 sensors, 4 on each jaw.

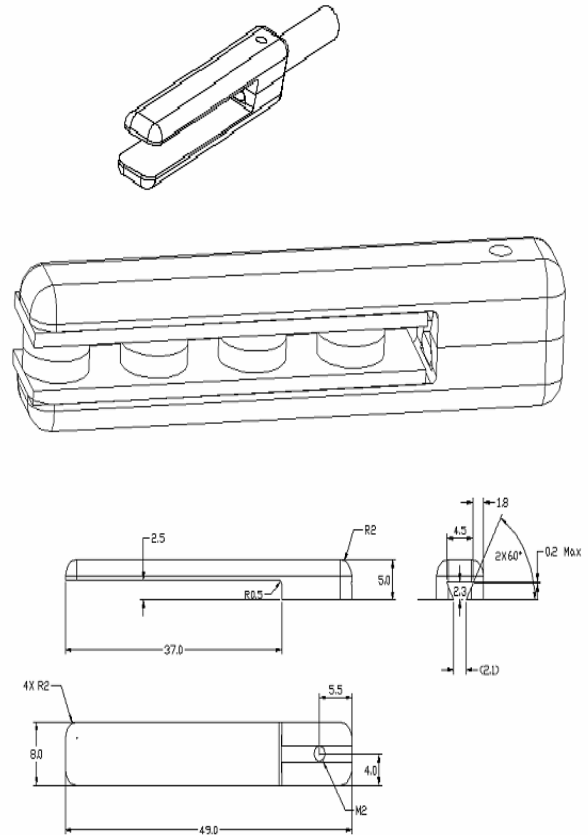


Fig. 6: Endoscope grasper mounting with the sensors and its detailed drawings. Dimensions are in mm.

As represented in the figure, we have a common substrate for all four sensors and they are integrated with the grasper jaw with the help of a dovetail fix that will slide into the grasper teeth. The object is grasped by both jaws with the sensors and the output from the eight sensors is fed to the in-house data acquisition system which is calibrated to visualize the softness of the different objects being grasped. After the objects are being tested by the sensors, the dovetail fix can be conveniently removed from the grasper teeth. Figure 7 presents a photograph of the designed assembly.

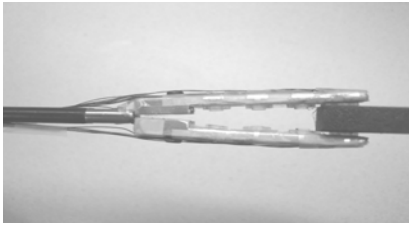


Fig. 7: Photograph of the endoscopic grasper integrated with 8 sensors.

RESULTS AND DISCUSSION

Various elastomeric-based objects with different tactile properties were grasped with the device and the experimental outputs were displayed using a gray coding method. For the sake of comparison, the softness of various elastomeric materials was experimentally measured using a standard durometer (ASTM D2240, type A and B). A number of experiments were conducted to determine the position and the size of the hard objects or lumps embedded within the soft elastomeric media. Following this, the position and size of the inclusion was determined and shown graphically. In Fig. 8, the grasper is touching an elastomeric object (with softness of 43 Shore). Here, only the two right hand sensors are engaged. The softness display shows the object in gray scale. Both the upper and lower sensor shows the same softness. This means that the grasped object has the same softness throughout its thickness, as expected.

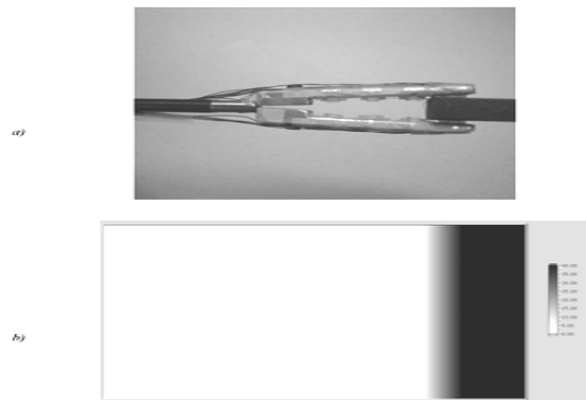


Fig. 8: a) Photograph of the endoscopic grasper touching an elastomeric object (with softness of 43 Shore). b) The softness display shows the object in gray scale.

The main target of the designed system was to detect the lumps within a medium. A number of runs

were conducted to determine the position and the size of the hard objects embedded within the soft elastomeric media. The hard objects were steel balls of various sizes. Using the designed system, the position and size of the inclusion was successfully determined and shown graphically. Figure 9 depicts the grasping of a soft medium in which steel balls are embedded.

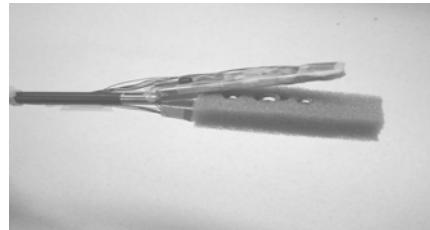


Fig. 9: A view of the grasper touching the elastomeric material with inclusions.

We showed that it is possible to localize lumps in two directions, along the jaw as well as along their depth. In this case, the object was sandwiched between two similar jaws and sensor arrays. The longitudinal location of the lumps can be found by comparing the outputs of each sensor array. The depth of the lumps can be determined by comparing the outputs of a sensing element in the lower jaw with its corresponding sensing element in the upper jaw, e.g., $2L$ & $2U$, which L and U stand for upper and lower jaws, respectively. The voltage amplitudes of each pair of sensing elements were proportional to the distances of the lump to those elements. For instance, for a particular case in which the lump was located exactly in the middle distance, the output voltages of both sensing elements of a pair were equal. To clarify the algorithm used for this study, we can consider the case illustrated in Fig. 10.

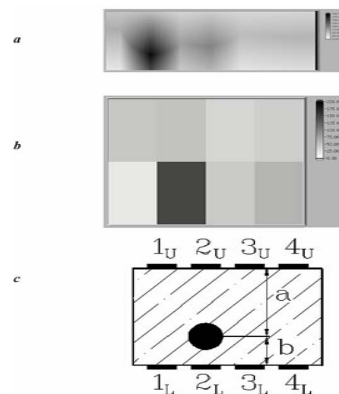


Fig. 10: Graphical rendering of the characterized lump in two dimensions.

This figure demonstrates a lump grasped by the grasper for which the location of the lump is aligned with the sensing elements $2U$ and $2L$. The distance of the lump to the upper and lower sensing elements are shown as a and b , respectively. The graphical representation is shown in the same figure. As can be seen, the lump is located somewhere between the sensors $2L$ and $2U$. Figure 10b shows the magnitude of the output signal from each sensor converted into intensity. For example, in Fig. 10c, the lump was placed directly over sensor $2L$. As a result, the output intensity of sensor $2L$ was higher than the other three sensors. However, this graph and with only two rows cannot demonstrate valuable information about the depth of the lump. To show the depth of the lump, the number of the graphical layers was increased to 100 by inserting 98 additional layers between the two original rows. It is assumed that the distances a and b are proportional to the number of layers located between the lump and the upper and lower surfaces, respectively. In other word, the sum of a and b is assumed to be equal to 100. The combination of these 100 layers and 4 sensing elements can be considered as a 100×4 matrix. Here, the intensity of each element in the matrix can be found by the procedure that follows. When an object is grasped, the output voltages of each sensor pair are read and compared together. In a special case, where the lump was placed at the same distance from the upper and lower surfaces, the equal output voltages from both sensing elements were anticipated. Thus, the intensity of the middle graphical layer, i.e., layer number 50, was set to the value $V_L + V_U$, in which V_L and V_U were the output voltages of the lower and upper sensing elements in each sensing pair, respectively. If the recorded voltages of a sensing pair were not equal, then the location of the lump could be found from the relationship: $a = (a+b) \times V_U / (V_L + V_U) = 100 \times V_U / (V_L + V_U)$. The distance of the lump from the lower surface, i.e., b , can simply be calculated knowing $b = 100 - a$. In this way, the location of the lump was determined. In order to find the size of the lump, we assigned the value $(V_U + V_L)$ to the central graphical element. Then, the values of the upper and lower elements were set to V_U and V_L . The enclosed elements were found using linear interpolation between these three known elements. To create a smooth transition between the columns, another interpolation between the adjacent columns was conducted by introducing arbitrary number of graphical columns. Figure 10a shows the lump position and its approximate size using this algorithm. The sample results of other tests of the lump detection and the corresponding experimental outputs are shown in Fig. 11.

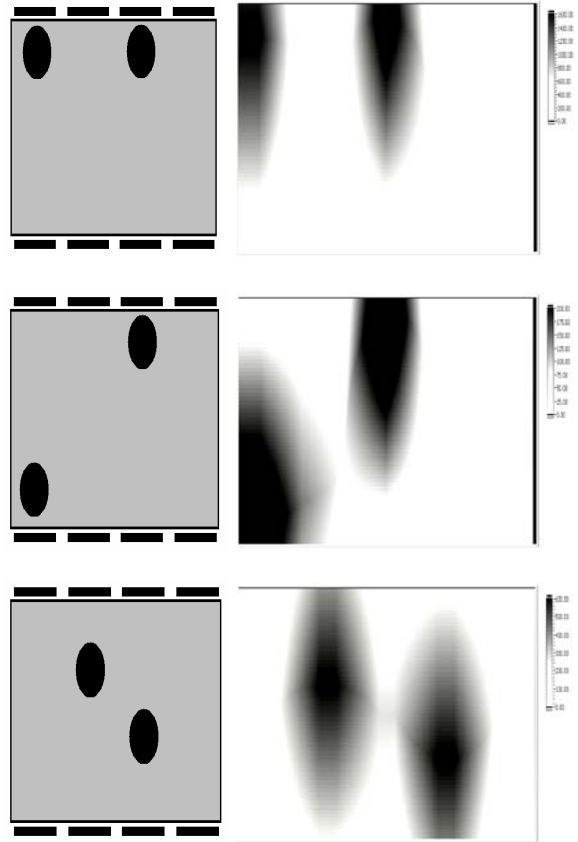


Fig. 11: Schematics of the lumps embedded within the elastomeric material. Grasping of the medium leads to the right-hand-side outputs.

Here, the schematics of the lumps embedded within the elastomeric material are shown on the left view. When the material is grasped by the grasper, the output is displayed which is shown on the right view.

CONCLUSION

The aim of this study was to develop an endoscopic grasper equipped with custom-designed micromachined tactile sensor targeted at detecting embedded objects. The microfabrication of a sensor capable of detecting the softness of a tissue was discussed in detail. Various processes involved in the construction of the final version of the sensor were also presented. The constructed sensors were incorporated into an endoscopic grasper and were subsequently used in the next stage of the study for detecting the embedded objects in a soft medium. A number of tests were conducted in order to investigate the performance

of the system. A gray scale coding technique was employed so that we could determine the size and location of the embedded lump. Our system has immediate medical application since the usual method of detecting the existence of a tumor in a biological tissue is to grasp the whole organ with a grasper or hand. Objects with known tactile properties were grasped with the device and the experimental outputs were compared with the known values. The average difference between the experimental data on softness and those obtained using the durometer was about 15%.

Due to the importance of pulse detection in biomedical engineering applications, work is currently underway in our lab to use the same system in pulse detection processes. The applications of the designed system are in detecting beating arteries in surgeries with minimal interventions.

ACKNOWLEDGEMENTS

The authors thank the Institute for Robotics and Intelligent Systems (IRIS), and the Natural Sciences and Engineering Research Council (NSERC) of Canada for providing partial financial support. We also would like to express our gratitude to the Center of Excellence of Biomedical Engineering of Iran based in Amirkabir University of technology, Faculty of Biomedical Engineering for its contribution. We also appreciate the support provided via the grant awarded by the Ministry of Health of Iran through Razi International Festival.

REFERENCES

1. Dario, P., 1991. Tactile Sensing-Technology and Applications. *Sensors and Actuators A-Physical*, 26(1/3): 251-261.
2. Dargahi, J., S. Najarian, 2004. Analysis of a Membrane Type Polymeric-Based Tactile Sensor for Biomedical and Medical Robotic Applications. *Sensors and Materials*, 16(1): 25-41.
3. Dargahi, J., S. Najarian, 2004. An Integrated Force-Position Tactile Sensor for Improving Diagnostic and Therapeutic Endoscopic Surgery. *Bio-Medical Materials and Engineering*, 14(2): 151-166.
4. Dargahi, J., 1998. Piezoelectric and Pyroelectric Transient Signal Analysis for Detecting the Temperature of an Object for Robotic Tactile Sensing. *Sensor and Actuators A-Physical*, 71(1/2): 89-97.
5. Dargahi, J., S. Najarian, K. Najarian, 2005. Development and 3-Dimensional Modeling of a Biological Tissue Grasper Tool Equipped with a Tactile Sensor. accepted for publication in *Canadian Journal of Electrical and Computer Engineering*.
6. Dargahi, J., S. Najarian, 2004. Theoretical and Experimental Analysis of a Piezoelectric Tactile Sensor for Use in Endoscopic Surgery. *Sensor Review*, 24(1): 74-83.
7. Fischer, H., B. Neisius, R. Trapp, 1995. *Interactive Technology and a New Paradigm for Health Care*. IOS Press, The Netherlands.
8. Howe, R.D., W.J. Peine, D.A. Kontarinis, J.S. Son, 1994. Remote Palpation Technology. *Proceedings of IEEE Engineering in Medicine and Biology Magazine*, 14(3): 318-323.
9. Bicchi, A., G. Canepa, D.De. Rossi, P. Iaconi, E.P. Scilingo, 1996. A Sensorized Minimally Invasive Surgery Tool for Detecting Tissue Elastic Properties. *Proceedings of IEEE International Conference Robotics and Automation*, Minneapolis, USA, 884-888.
10. Brouwer, I., J. Ustin, L. Bentley, A. Sherman, N. Dhruv, F. Tendick, 2001. Measuring in vivo Animal Soft Tissue Properties for Haptic Modeling in Surgical Simulation. In *Studies in Health Technology Informatics - Medicine Meets Virtual Reality*, Amsterdam: ISO Press, 69-74.
11. Dargahi, J., S. Najarian, 2004. A Supported Membrane Type Sensor for Medical Tactile Mapping. *Sensor Review*, 24(3): 284-297.
12. Hannaford, B., J. Trujillo, M. Sinanan, M. Moreyra, J. Rosen, J. Brown, R. Leuschke, M. MacFarlane, 1998. Computerized Endoscopic Surgical Grasper. In *Studies in Health Technology Informatics-Medicine Meets Virtual Reality*, Amsterdam, ISO Press, 265-271.
13. Dargahi, J., S. Najarian, 2004. Human Tactile Perception as a Standard for Artificial Tactile Sensing-a review. *International Journal of Medical Robotics and Computer Assisted Surgery*, 1(13): 23-35.
14. Dargahi, J., S. Najarian, 2005. Advances in Tactile Sensors Design/Manufacturing and Its Impact on Robotics Applications- a review. *Industrial Robot*, 32(3): 268-281.
15. Dargahi, J., S. Najarian, 2003. An Endoscopic Force Position Grasper with Minimum Sensors. *Canadian Journal of Electrical and Computer Engineering*, 28(3/4): 155-161.

16. Dargahi, J., S. Najarian, X.Z. Zheng, 2005. Measurements and Modeling of Compliance Using a Novel Multi-Sensor Endoscopic Grasper Device. *Sensors and Materials*, 17(1): 7-20.
17. Dario, P., M.C. Carrozza, L. Lencioni, B. Magnani, S. D'Attanasio, 1997. A Micro Robotic System for Colonoscopy. *Proc. IEEE Int. Conf. on Robotics and Automation*, IEEE Robotics and Automation Society, 1567-1572.
18. Lee, M.H., H.R. Nicholls, 1999. Tactile Sensing for Mechatronics-A State-of-the-Art Surgery. *Mechatronics*, 9(1): 1-31.
19. Bar-Cohen, Y., C. Mavroidis, M. Bouzit, B. Dolgin, D. Harm, G. Kopchok, R. White, 2000. Virtual Reality Robotic Operation Simulations Using MEMICA Haptic System. *Proc. Int. Conf. for Smart Systems and Robotics for Medicine and Space Applications*, Houston, USA.
20. Sakas, G., 2002. Trends in Medical Imaging: from 2D to 3D. *Computers and Graphics*, 26: 577-587.
21. Fisch, A., C. Mavroidis, J. Melli-Huber, Y. Bar-Cohen, 2003. Haptic Devices for Virtual Reality, Telepresence, and Human-Assistive Robotics. chap. 4 in *Biologically-Inspired Intelligent Robots*, Bellingham, Wash.
22. Dargahi, J., M. Parameswaran, S. Payandeh, 2000. A Micromachined Piezoelectric Tactile Sensor for Endoscopic Grasper-Theory, Fabrication, and Experiments. *Journal of Microelectromechanical Systems*, 9(3): 329-335.
23. Melzer, H.H., M.O. Schurr, W. Kunert, G. Buess, U. Voges, J.U. Meyer, 1993. Intelligent Surgical Instrument System. *Endoscopic Surgery and Allied Technologies*, 1(3): 165-170.
24. Tanase, D., J.F.L. Goosen, P.J. Trimp, P.J. French, 2002. Multi-Parameter Sensor System with Intravascular Navigation for Catheter/Guide Wire Application. *Sensors and Actuators A*, 97-98: 116-124.
25. Tanase, D., J.F.L. Goosen, P.J. Trimp, P.J. French, 2000. System for Localization and Guidance of Catheters. *Proceedings of SMIT*, Gelsenkirchen, Germany.
26. Tanase, D., P.J. French, J.F.L. Goosen, P.J. Trimp, J.A. Reekers, 2000. Catheter Navigation System for Intravascular Use. *Proceedings of the IEEE-EMBS Special Topic Conference on Microtechnologies in Medicine and Biology*, Lyon, France.
27. Burger, F., P.A. Besse, R.S. Popvic, 1998. New Fully Integrated 3D Silicon Hall Sensor for Precise Angular-Position Measurements. *Sensors and Actuators A*, 67: 72-76.
28. Regelsberger, J., F. Lohmann, K. Helmke, M. Westphal, 2000. Ultrasound-Guided Surgery of Deep Seated Brain Lesions. *European Journal of Ultrasound*, 12(2): 115-121.
29. Lundgren, M., 2003. Path Tracking and Obstacle Avoidance for a Miniature Robot. Master Thesis, Umea University, Sweden.
30. Dargahi, J., 1993. The Application of Polyvinylidene Fluoride as a Robotic Tactile Sensor. Ph.D. dissertation, Glasgow Caledonian University, Glasgow, Scotland.
31. Fearing, R.S., G. Moy, E. Tan, 1997. Some Basic Issues in Teletaction. *Proceedings of IEEE International Conference on Robotics and Automation*, Albuquerque, USA, 3093-3099.
32. Dargahi, J., 2000. A Three Sensing Element Piezoelectric Tactile Sensor for Robotic and Prosthetic Applications. *Sensors and Actuators A-Physical*, 80(1): 23-30.
33. Dargahi, J., 2002. An Endoscopic and Robotic Tooth-Like Compliance and Roughness Tactile Sensor. *Journal of Mechanical Design*, 124: 576-582.
34. Geisthoff, W., S.H. Tretbar, P.A. Federspil, P.K. Plinkert, 2004. Improved Ultrasound-Based Navigation for Robotic Drilling at the Lateral Skull Base. *International Congress Series*, 1268: 662-666.
35. Strommer, G., L. Schwartz, I. Shmarak, M.Y. Flugelman, A. Shiran, L. Sobe, E. Oren, R. Shofti, M.B. Leon, B.S. Lewis, 2005. Fluoroscopy-Free Navigation of Guided-Stent Using Medical Positioning System and 3D Guided-IVUS Image. *International Congress Series*, 1281: 387-392.
36. Mirbagheri, A., J. Dargahi, S. Najarian, F. Tabatabai Ghomshe, 2007. Design, Fabrication, and Testing of a Membrane Piezoelectric Tactile Sensor with Four Sensing Elements. *American Journal of Applied Sciences*, 4 (9): 645-652.